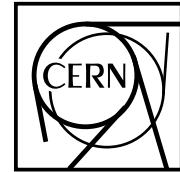




The Compact Muon Solenoid Experiment

# CMS Note

Mailing address: CMS CERN, CH-1211 GENEVA 23, Switzerland



## Effect of the tracker cables on the photon resolution in CMS ECAL

K. Lassila-Perini

*Institute of Particle Physics (IPP), ETHZ, CH-8093 Zürich, Switzerland*

### Abstract

The effect of the tracker cables going through the gap between the tracker and the electromagnetic calorimeter has been studied. Three different cable arrangements have been investigated using 85 GeV photons at  $\eta=1.25$ . The optimal solution is when the cables are uniformly distributed and placed as close as possible to the electromagnetic calorimeter.

# 1 Introduction

The excellent photon resolution of the CMS lead tungstate electromagnetic calorimeter may deteriorate if the photons convert into an electron-positron pair in the material after the measuring tracker layers. Such photons will lose energy and generate a tail in the photon resolution. Figure 1 shows the distribution of the reconstructed energy of photons in three different  $\eta$  ranges for non-converted photons[1] and for late conversions (conversion happens at a radius larger than 115 cm, the tracker layers end at 120 cm). The photons have the energy spectrum and rapidity of the decay photons of 100 GeV Higgs and the energy has been normalised to the initial energy of the photon. The energy is measured in 5x5 crystals around the crystal with the maximum energy deposit. The degradation of the energy measurement is clearly visible, and it is more pronounced in the high  $\eta$  range where there are more cables and where the photon track in the cable material is longer.

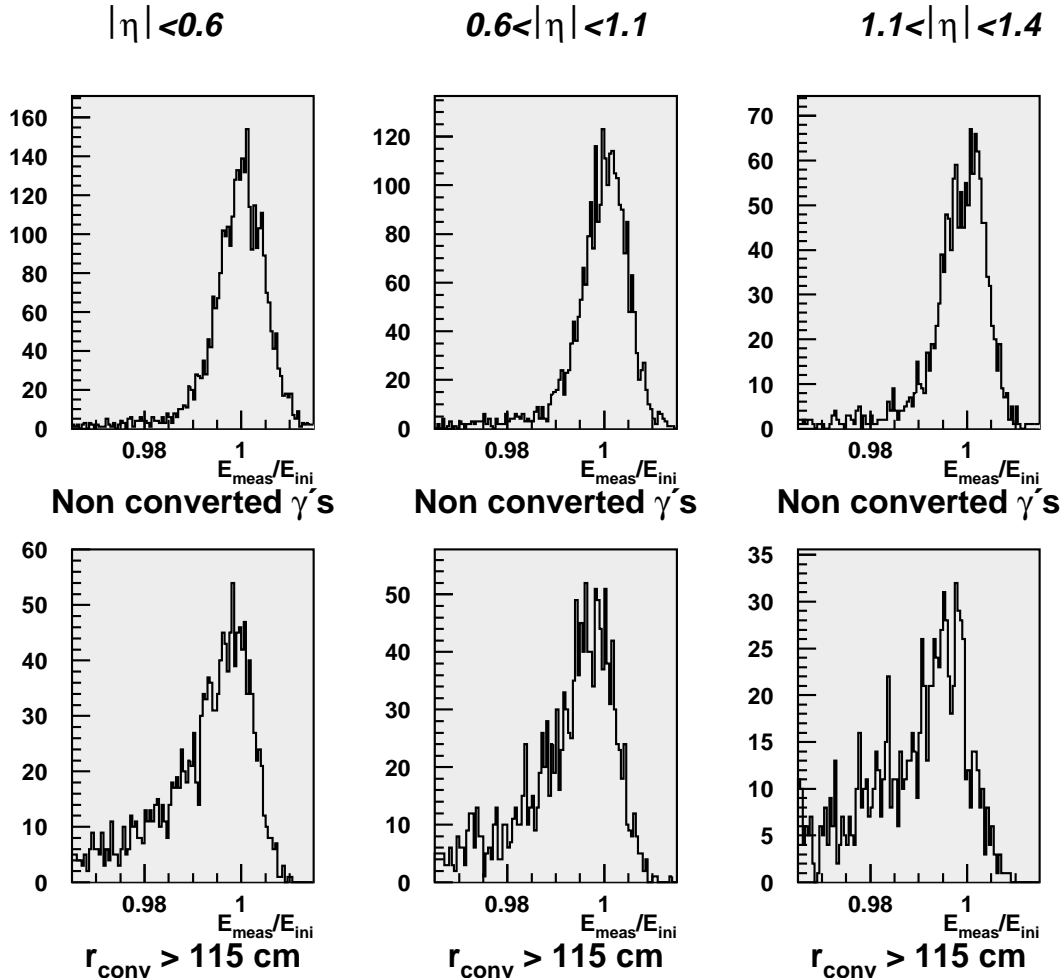


Figure 1: The energy distribution normalised to the incident energy of photons from the decay of a Higgs boson with a mass of 100 GeV. The distributions for non-converted photons[1] are shown on the top and the distributions for photons that convert late ( $r > 115$ cm) are shown below. The active part of the tracker ends at 120cm.

For such photons the tracker information cannot be used to tell that they have converted as is the case for early conversions where the electron-positron pair leaves tracks in the tracker. Therefore it is important to assure that the late conversions look like normal photons that do not interact before the electromagnetic calorimeter.

## 2 Simulation setup

The simulation study uses CMSIM008[2] package, with a detailed description of the tracker as defined in the CMS technical proposal[3] and the crystal geometry[4]. The part defining the cables in the tracker geometry has been modified: three cable geometries have been used to find the optimal solution from the point of view of photon energy resolution. In all cases the cable volume is kept constant. The cable material consists of aluminium, polyethylene,

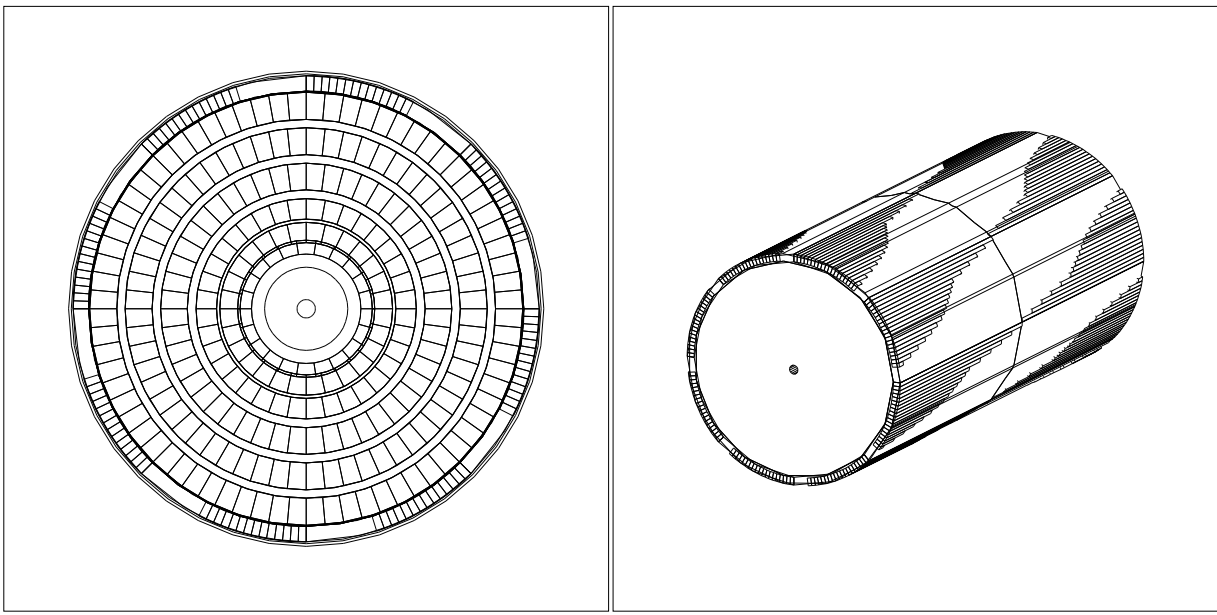


Figure 2: The default configuration for the cables

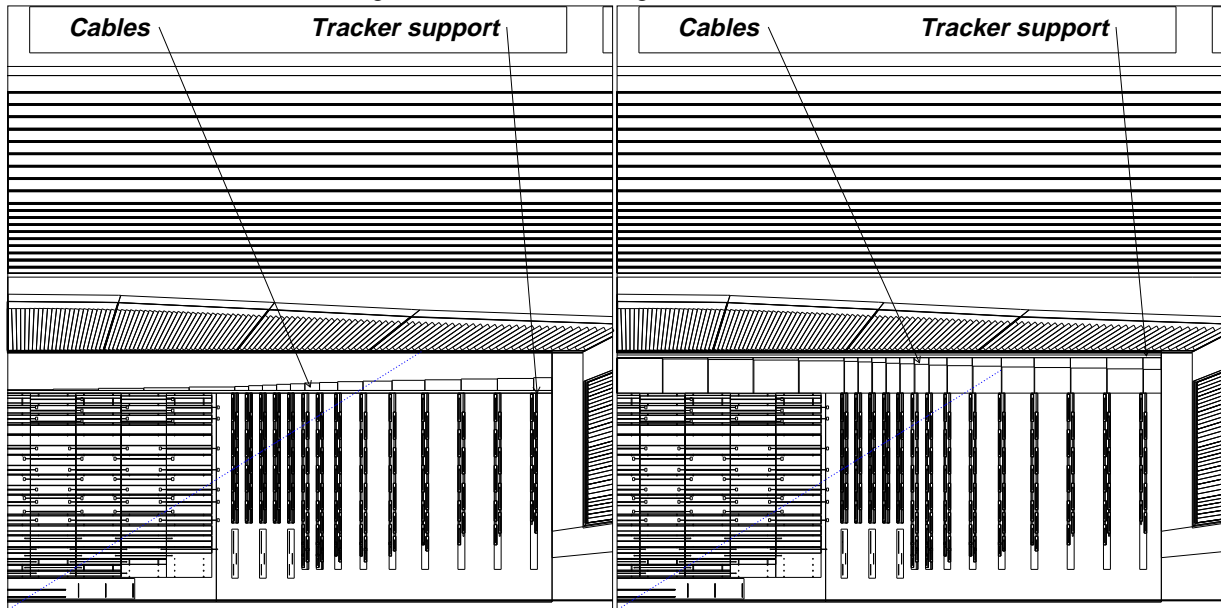


Figure 3: The modifications: to the left: 1st modification, cables uniform in  $\phi$  and close to the tracker; to the right: 2nd modification, cables uniform in  $\phi$  and close to the crystals. The line indicates the direction of  $\eta=1.25$ .

optical fibres and cooling fluids and it is approximated by a uniform mixture with an average atomic weight of  $A = 18$  and an average atomic number of  $Z = 9$ . The average density is estimated to be  $2.2 \text{ g/cm}^3$  and the radiation length  $X_0 = 14.1 \text{ cm}$ .

In the default case[5] the cables are not uniform in  $\phi$  but are combined in 8 segments. From each tracker wheel a new bunch of cables is added to segments. The depth ( $r_{max} - r_{min}$ ) of the cables is constant in every wheel. The 1.5 cm tracker support lays outside the cables (see Figure 2).

In the first modification (Figure 3) the tracker support structure is brought inside the cables. The cables are uniform in  $\phi$  and the maximum radius of the cables at each wheel is defined so that the cable volume stays the same as in the default case.

In the second modification (Figure 3) the tracker support is brought up to 2 cm from the ECAL support and the cables are placed just inside the support tube. The minimum radius of the cables at each wheel is defined so that the cable volume stays the same as in the default case.

The main parameters of the three different options are shown in the table 1. The ECAL support plate starts at  $r = 143$  cm and the crystals are positioned on a cylinder with  $r = 144$  cm.

		Default	1st modification	2nd modification
Tracker support	$r_{min}$	129.5 cm	120.0 cm	139.5 cm
	$r_{max}$	131.0 cm	121.5 cm	141.0 cm
Cables	$r_{min}$	120.0 cm	121.5 cm	defined by volume
	$r_{max}$	128.5 cm	defined by volume	139.5 cm

Table 1: Main parameters of the three cable geometries

To study the differences, samples 85 GeV photons at  $\eta = 1.25$  have been simulated. 85 GeV is the most probable decay photon energy from 100 GeV Higgs around this  $\eta$  value. Only the photons converting between  $r = 115$  cm and the ECAL support structure (143 cm) are simulated. The electromagnetic shower is fully simulated with GEANT3.21[6] and the energy cut below which particles are stopped is 100 keV. Using lower cuts would not change the results essentially. The non-uniform longitudinal light transmission in the crystals is taken into account in the simulation. The noise or the fluctuations due to the light transport are not added to the simulation results. This additional fluctuation is the major contribution to the width of the distribution but, as it has Gaussian form, the tails of the distribution will remain even when it is added.

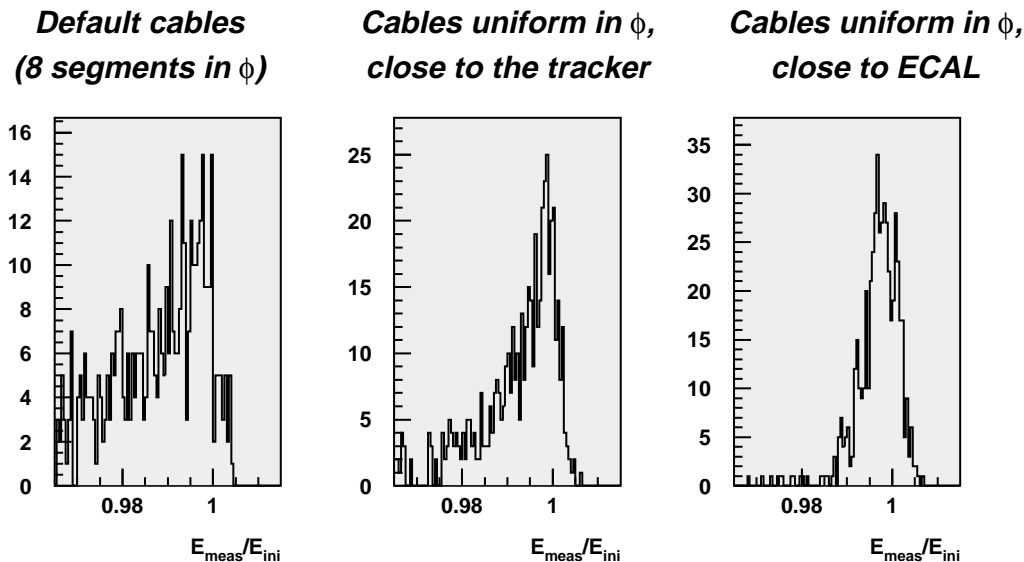


Figure 4: The energy distribution of 85 GeV photons at  $\eta = 1.25$  converting late in the tracker ( $r > 115$ cm) for three different cable geometries.

### 3 Results

The energy of the converted photons is measured in an array of 5x5 crystals around the one containing the maximum energy deposit. Figure 4 shows the photon energy distribution normalised to the incident energy for the three different cable arrangements. The low-energy tail is very pronounced in the default case. In the first modification where the cables are uniform in  $\phi$  but far from the crystals, the tail diminishes but does not disappear. In the second modification where the air gap between the cables and the crystal is reduced, the tail disappears. The fraction of the events contained within  $\pm 1, 2$  and  $3$  Gaussian  $\sigma$ 's of the non-converted photons ( $\sigma=0.27\%$ ) is shown in table 2 for the non-converted photons and for the late conversions in the three cable geometries. The efficiency of the late conversions in the second modification is only slightly worse than that of non-converted photons and clearly better than in the other configurations. The reasons for the improvement can be studied by considering the energy

deposited in the cables.

	Non converted $\gamma$ 's	Default	1st modification	2nd modification
$\pm 1\sigma$	54.2%	15.1%	32.7%	43.6%
$\pm 2\sigma$	78.2%	28.2%	48.5%	70.8%
$\pm 3\sigma$	85.4%	36.6%	59.2%	84.5%

Table 2: Fraction of the events contained within 1, 2 and 3 Gaussian  $\sigma$ 's for the non-converted photons and for the late conversions in the three different cable arrangements. In each case  $\sigma$  of the distribution for non-converted photons is used and the window is centred at its mean value.

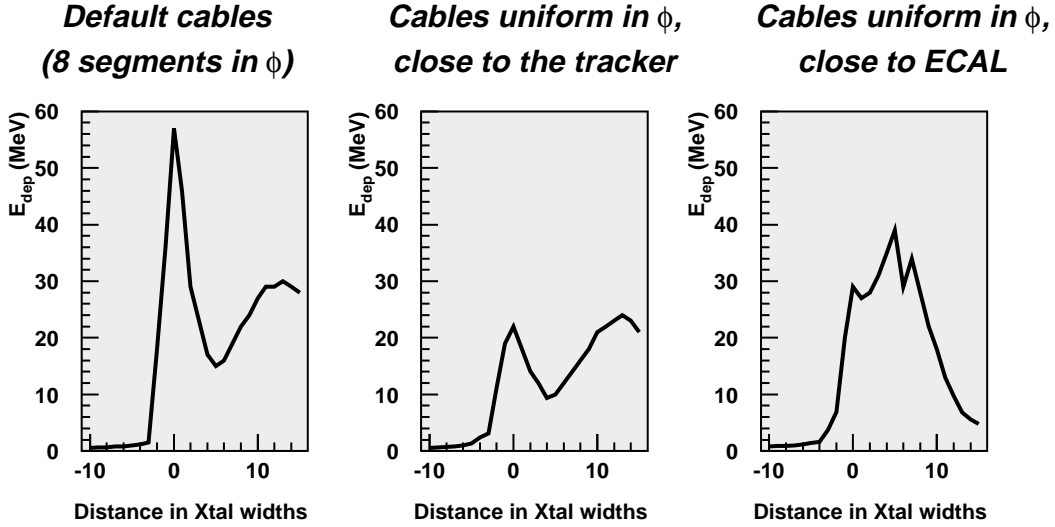


Figure 5: The energy deposit of 85 GeV converted photons in the tracker cables. The cables have been divided into  $\eta$ -bins, each bin corresponding to the crystal width. The distance is measured from the photon incident direction and the positive direction of the x-axis corresponds to the increasing  $\eta$ . The total energy deposit in the cables is 0.69 GeV for the default case and 0.45 GeV and 0.44 GeV respectively for the two modifications.

The energy deposit in the cables is recorded. The cable is divided into bins in  $\eta$ , each bin with a width of  $\Delta\eta = 0.0145$  i.e. the width of the crystal. In figure 5 the energy deposit in the cables is plotted as a function of the distance in crystal widths from the photon direction. In the default case, the energy deposit is highest in the area where the photon hits the cables but it rises again several crystal widths away from the hit. This is due to the low energy secondary particles generated in the cable material that curl in the air gap due to the 4T magnetic field. If they do not have enough energy to reach the crystals they curl back to the cables and deposit their energy in the cables far away from the incident point.

In the first modification, the energy deposited in the cables is less than in the default case: the total energy deposit is 0.45 GeV instead of 0.69 GeV of the default case. This is due to the fact that the converted photon sees less material as the cables are uniformly distributed in  $\phi$ . However, the energy deposit far from the interaction point is not reduced.

In the second modification, the energy deposit in the cables is concentrated around the impact point and some crystal widths towards high  $\eta$ . There is much less energy deposit far away from the hit as in the two other cases. This is due to the reduced air gap (2 cm); the secondary particles that curl in the magnetic field will hit the crystals instead of bending back into the cables. The total energy deposit in the cables is 0.44 GeV.

## 4 Conclusions

It is shown that the air gap between the tracker cables and the electromagnetic calorimeter has to be as small as possible. Otherwise the secondary particles from the interactions in the cables curl in the magnetic field and their energy will be lost in the cables at a point away from the impact point. The amount of energy lost in the cables can also be reduced by placing the cables uniformly in  $\phi$ , but this is not enough to reduce the leakage towards high  $\eta$ : the air gap is the main reason for the degradation of the energy measurement.

## 5 Acknowledgements

I am grateful to Tejinder Virdee and Chris Seez for many useful discussions and I thank Rui Ribeiro for his help with the CMS tracker geometry software.

## References

- [1] K. Lassila-Perini: Technical note in preparation
- [2] CMS TN/93-63 CMSIM-CMANA CMS Simulation Facilities
- [3] CERN/LHCC 94-38 CMS Technical Proposal
- [4] CMS-TN 95-151 J-P. Vialle, M. Lebeau, A. Givernaud, M. Maire: Barrel ECAL simulation and optimization in CMS
- [5] R. Ribeiro, J. Stefanescu: tracker version 4 in CMSIM008
- [6] CERN Program Library Long Writeup W5013